Advanced Studies in Biology, Vol. 8, 2016, no. 1, 27 - 38
HIKARI Ltd, www.m-hikari.com
http://dx.doi.org/10.12988/asb.2016.611

Drift Coefficient and Simulation of Amino Acid-Solvent Interactions for Proteins whose Main Chain Have α-Helical Secondary Structures

Wilson I. Barredo*

Department of Physics
Mindanao State University (MSU)-Iligan Institute of Technology
Iligan City, 9200 Philippines
&
Department of Physics, Mindanao State University
Marawi City, 9700 Philippines
*Corresponding author

Henry P. Aringa

Department of Physics, Mindanao State University
Marawi City, 9700 Philippines

Abstract

The formation of multiple helical-linear segments of a polymer in a solvent is investigated analytically. Winding probability functions for diffusive polypeptides is obtained for a drift coefficient $f(s)$ involving Fourier cosine function of the variable s along the chain. Applications to protein chains are explored where the formation of α-helices between linear segments is compared to the conformation of myoglobin (4mbn) found in the Protein Data Bank (PDB). The results generated are also comparable to the results of the well-known APSSP2 secondary structure prediction server of Raghava which employed a sophisticated Example Based Learning (EBL) approach with a combination of neural network and nearest neighbour algorithm. Considering the large amount of data from Protein Data Bank (PDB), we can conveniently predict or mimic the structure of

other α-helical proteins in solvents with much less computing times which can be used to explore the protein folding problem.

Keywords: drift coefficient, winding probability, diffusive polypeptides, secondary structure, helix-turn-helix

1 Introduction

Predicting, modeling, and understanding the dynamics of the native structure of proteins have been topics of intense interdisciplinary investigation. The primary goal has been to gain a deeper understanding of why and how proteins acquire specific conformations that allow them to perform various biological functions. For instance, the application of computational methods has shown successes in simulating the folding of proteins [1, 2]. However, employing more realistic potentials or an all-atom simulation for the folding process is constrained by computing time and resources which often limit the study to short polypeptide chains [3, 4]. The daunting task of understanding and predicting conformations of thousands of proteins requires that a variety of approaches to understand protein folding be explored.

A newly synthesized protein starts as an unfolded linear chain of amino acids. The transition from a randomly coiled polypeptide to a unique three-dimensional structure, however, normally occurs in a crowded living cell where each amino acid in the chain has to diffuse through the aqueous environment before attaining a specific position in the protein's native state. Aside from interactions among amino acids of a protein, the role of the solvent is also crucial [5, 6]. Since a monomer may be hydrophobic or hydrophilic, and positively or negatively charged, among other properties, the value of the drift coefficient varies from segment to segment for a polypeptide chain diffusing in an aqueous medium.

This paper investigate the problem by viewing the conformation of myoglobin (4mbn) as arrays of diffusion paths modulated by Fourier cosine function (Eq. (12)) as drift coefficient in order to predict the structure of this α-helical protein and at the same time also identify the amino acid sequence on the helical segments.

2 Probability Density for Winding Polypeptides

The solution of the Fokker-Planck equation for small intervals of time, $\tau \ll 1$, is given by the conditional probability density [7, 8, 9]

$$\mathrm{P}\left(\boldsymbol{r},\ t+\tau \mid \boldsymbol{r_0}, t\right) = \left(\frac{1}{2\pi D\tau}\right)^{3/2} \exp\left\{-\frac{1}{2D}\left[\left(\frac{\Delta \boldsymbol{r}}{\tau}\right) - \boldsymbol{A}\right]^2 \tau\right\}. \qquad (1)$$

Where $\mathbf{A}\ (r_0, \mathrm{t})$ is the drift vector, and D a constant diffusion coefficient. Denoting the length travelled in time $\tau \ll 1$ as $\Delta s = v\tau$, where v is the average speed of the random motion [10], Eq. (1) acquires the form,

$$\mathrm{P}\,(\boldsymbol{r},\ s_0+\Delta s\,|\boldsymbol{r_0},s_0)=\left(\frac{\nu}{2\pi D\Delta s}\right)^{3/2}\exp\left\{-\frac{\nu}{2D}\left[\left(\frac{\Delta r}{\Delta s}\right)-\frac{\boldsymbol{A}}{\nu}\right]^2\Delta s\right\}, \tag{2}$$

with, $\Delta s << 1$. Application of the Chapman-Kolmogorov equation leads to a conditional probability density given by the path integral,

$$\mathrm{P}\,(\boldsymbol{r}_1,\mathrm{L}\mid\boldsymbol{r_0},0)=\int exp\left\{-\frac{3}{2l}\int_0^L\left[\frac{dr}{ds}-\frac{l}{3D}\,\boldsymbol{A}\right]^2 ds\right\}D[\boldsymbol{r}]\ , \tag{3}$$

where, l= 3D/v, which has a dimension of length, L is the total path length and the integral is taken over all paths r(s) starting at r(0) = r_0 and ending at r(L) = r_1 , with $0 \leq s \leq L$.

We shall now use the path integral, Eq. (3), to model a polypeptide chain where various paths with endpoints at r_0 and r_1 are viewed as possible conformations of a biopolymer with the same endpoints. For the chain-like macromolecule, N would be the number of amino acids, each taken to be of length l. Trajectories of the path integral would consist of N steps each of length l, such that L= Nl is the length of the polymer [11, 12, 13]. The path of Eq. (3) can be parametrized as,

$$\boldsymbol{r}\,(\mathrm{s}) = \boldsymbol{r_c} + \kappa\,\mathbf{B}\,(\mathrm{s}), \tag{4}$$

where $\boldsymbol{r_c}$ is the classical path, and **B** (s) are the Brownian fluctuations about $\boldsymbol{r_c}$ with κ a constant. The derivative of the path **r** (s) is given by, dr/ds = $\kappa\,\omega(s)$, where $\omega(s)$ = d**B**/ds is a Gaussian random white noise variable [14, 15, 16]. The evaluation of this variable makes use of the method introduced by Hida and Streit [14, 15, 16, 17] for the quantum mechanical propagator.

3 Winding Probability for Helical Conformations

It is convenient to use circular cylindrical coordinates in discussing helical structures where r = (ρ, ϑ, z). In a discussion of a polymer represented by a random walk, F. W. Wiegel [13] showed that a potential V(ρ) induces a polymer to wind around the z-axis at a distance $\rho = R$, where R is a minimum of the potential. A close look at α −helix does show that the amino acid side chains extend outward from the helical backbone, the interaction of the side chains with the aqueous environment may contribute to a radial potential V(ρ).

In view of the axial symmetry, we can simplify the study of the winding behavior of a biopolymer by projecting the paths on the $\rho - \vartheta$ plane. One then considers a chain which lies on the plane perpendicular to the z-axis, with endpoints at ρ_0 = (ρ_0, ϑ_0) and ρ_1 = (ρ_1, ϑ_1). From this scenario, a polymer which winds around the z-axis due to a potential V(ρ) with a minimum at $\rho = \boldsymbol{R}$, projects a circular structure on the $\rho - \vartheta$ plane. In this case, a conditional probability density with $\rho = (\boldsymbol{R},\ \vartheta)$, can be given by:

$$\mathrm{P}\,(\vartheta_1, \vartheta_0) = \int exp\left\{-\frac{1}{l}\int_0^L \left[\frac{d\vartheta}{ds} - \frac{l}{2D}\, f\,(s)\right]^2 ds\right\} D[\boldsymbol{\vartheta}], \tag{5}$$

We let **A** = (0, *f*(*s*), 0) where *f*(*s*) is the ϑ - component of the drift vector. To reflect the varying interactions of the different amino acids in an aqueous environment, the value of the drift coefficient *f*(*s*), with $0 \leq s \leq L$, can also vary at each length segment along the chainlike molecule. Corresponding to Eq. (4), ϑ can be parametrized as

$$\vartheta\,(s) = \vartheta_c + (\sqrt{l}/\mathrm{R})\, B\,(\mathrm{s}) \tag{6}$$

where ϑ_c is the classical trajectory, and *B* the Brownian fluctuation.

Eq. (5) deals with paths confined to a circular topology. The paths can be classified topologically and characterized by winding numbers [10, 11, 12], [19]-[22] n= 0, $\pm1, \pm2, \ldots$ where, n > 0 signifies n turns counterclockwise around the origin; n < 0 means $|n|$ turns clockwise, and n = 0 signifies no winding [23]. An evaluation of Eq. (5) yields the result [7, 18],

$$P\,(\vartheta_1, \vartheta_0) = \sum_{n=-\infty}^{+\infty} P_n, \tag{7}$$

where,

$$P_n = \sqrt{\frac{R^2}{\pi lL}}\ \exp\left[-\frac{R^2}{lL}\left(\vartheta_0 - \vartheta_1 + 2\pi n + \frac{l}{2DR}\int_0^L f\,(s)ds\right)^2\right]. \tag{8}$$

Eq. (8) is just the probability function for n-times winding of a path around the z-axis. Alternatively, the probability function can be written as,

$$P(\vartheta_1, \vartheta_0) = \frac{1}{2\pi}\sum_{m=-\infty}^{+\infty} \exp\left(-\frac{lL}{4R^2}\, m^2\right) \times \exp\left\{-im\left[(\vartheta_0 - \vartheta_1) + \frac{1}{2DR}\int_0^L f\,(s)ds\right]\right\} \tag{9}$$

The probability that a helical conformation has a polypeptide winding n-times about the z-axis is given by, *W (n, L)* = P_n/P. For an arbitrary initial point, we let $\vartheta_0 = \vartheta_1$, and with Eqs. (8) and (9) we obtain,

$$W(n, L) = R\sqrt{\frac{4\pi}{lL}}\ \frac{exp\left[-\frac{R^2}{lL}\left(2\pi n + \frac{l}{2DR}\int_0^L f\,(s)ds\right)^2\right]}{\theta_3\left(\frac{1}{4DR}\int_0^L f\,(s)ds\right)}, \tag{10}$$

where $\theta_3\,(u)$ is the theta function [24]. We note that Eq. (10) is a full and exact result obtained by evaluating Eq. (5). The interaction of each amino acid with the aqueous environment as well as with other monomers would be reflected in the drift coefficient *f*(*s*), as s ranges from 0 to L along the length of a biopolymer. The *f*(*s*) in turn serves as a modulating function affecting the winding probability W (*n, L*) that describes a specific winding conformation.

The winding probability of a very long polymer chain; that is L >> 1, $\theta_3(u) \approx 1$, on the x-y plane that winds n-times around the z-axis (that is, forming a helical configuration) is given by

$$W(n,L) = \sqrt{\frac{4\pi R^2}{lL}} \exp\left\{-\frac{R^2}{lL}\left(2n\pi + \frac{l}{2DR}\int_0^L f(s)ds\right)^2\right\} \quad (11)$$

where R is the radius of the helix and $L = Nl$, the length of the polymer with monomer length l and number of monomer N, and n is the number of helical turns. The function $f(s)$ is called the drift coefficient and D, the diffusion constant.

The winding probability Eq. (11) explicitly depends on the drift coefficient $f(s)$, as s ranges from 0 to L along the length of the polymer. The length-dependent drift function $f(s)$ can take any integrable function. It has different forms of function that had been considered so far, such as $f(s) = K\cos(vs)$ [25, 26] which was used to model a sequence of bases where the purines alternate with the pyrimidines along the DNA strand were approximated with this sinusoidal function, where ν is the frequency of the repeating unit and K is constant; $f(s) = KL_2(vs)$ [26, 28] which was used to model sequence of monomers in a polymer; and the Besselian drift coefficient $f(s) = KJ_{2p+1}(vs)$ [27, 28, 30] which was used to model the structures of several alpha-helical proteins to obtain an empirical formula that can predict the diffusion coefficients of alpha-helical proteins in solvents.

4 Drift Coefficient

The drift coefficient $f(s)$ can simulate the interaction of each monomer of a protein with its aqueous environment as well as with other monomers. Which means that $f(s)$ also acts as a modulating function affecting the winding probability $W(n, L)$ which in turn describes a specific winding conformation. We present in this paper a drift coefficient that can closely predict the structure of alpha helical proteins and can also closely identify the amino acid sequence on the helical segments that is of the form,

$$f(s) = k\sum_{q=1,3,5,\ldots}^{p} \cos(qvs) \quad (12)$$

where k and v are constants. Integrating Eq. (12) over ds, we get

$$\int_0^L f(s)ds = \frac{k}{v}\sum_{q=1,3,5,\ldots}^{p} \frac{\sin(qvL)}{q}. \quad (13)$$

Hence; if we substitute Eq. (13) into Eq. (11), the winding probability can be written in the form,

$$W(n,L) = \sqrt{\frac{4\pi R^2}{lL}} \exp\left\{-\frac{R^2}{lL}\left(2n\pi + \frac{lk}{2vDR}\sum_{q=1,3,5,\ldots}^{p} \frac{\sin(qvL)}{q}\right)^2\right\}. \quad (14)$$

As an application, we will consider the α-helical protein myoglobin (4mbn) as example to demonstrate that with the correct choice of drift function such as Eq. (12) we can predict the structure of α-helical proteins and can also identify the amino acid sequence on the helical segments.

Myoglobin (4mbn) has a total length of 153 residues, α-helical segments is about 80% of its length or about 123 residues, and has 11 helices [29]. For the values R = 0.25 nm, l = 0.15 nm, and 3.6 residues/turn typical of an α-helix, we will then know that 4mbn has n = -(123 residues)/(3.6 residues/turn) ≈ -34 helical turns and a length of L = 0.15(153) nm ≈ 23 nm. Then plotting the winding probability Eq. (14) using the above data and with k/D = 1346/nm, v = 1.527/nm, and choosing p = 89 gives us a helix-turn-helix graph presented in Figure 1. The negative value for the number of turn n signifies that this protein is right-handed. Take note also that the values for k/D and v were generated using the empirical formula that we have established and the technique that we have develop on our earlier work on diffusion of proteins in solvents [30].

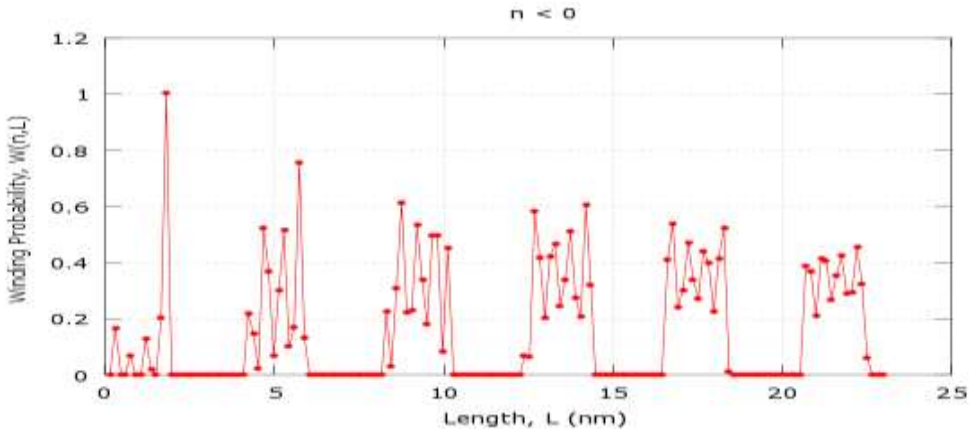

Figure 1: 4MBN: Graph of W(-n, L) versus length (L) were each dot represent an amino acid

On the other hand, myoglobin (4mbn) has the following sequence of amino acids [31]:

(VLSEGEWQLVLHVWAKVEADVAGHGQDILIRLFKSHPETLEKFDRFKHLKTEAEMKASE
DLKKHGVTVLTALGAILKKKGHHEAELKPLAQSHATKHKIPIKYLEFISEAIIHVLHSRHPGDFGA
DAQGAMNKALELFRKDIAAKYKELGYQG)

And in Figure 1, the helix-turn-helix structure we predicted for this protein is presented. The helical segments are the amino acids (sequence of amino acids)

with none-zero winding probability and the turn segments are the amino acids (sequence of amino acids) with winding probability W(-n, L) = 0. As can be seen in the figure above, there are about six major helical segments with amino acid sequence:

1)LSEGEWQLVLHV 2)DILIRLFKSHPET 3)AEMKASEDLKKHGVT 4)HEAELKPLAQSHATKH
5)AIIHVLHSRHPGDFG 6)LFRKDIAAKYKELGY.

Or the helix-turn-helix structure will look like this one:

```
.hhhhhhhhhhhh............hhhhhhhhhhhhh............hhhhhhhhhhhhhhh......
VLSEGEWQLVLHVWAKVEADVAGHGQDILIRLFKSHPETLEKFDRFKHLKTEAEMKASEDLKKHGVTVLTALG

........hhhhhhhhhhhhhhhh............hhhhhhhhhhhhhh............hhhhhhhhhh
AILKKKGHHEAELKPLAQSHATKHKIPIKYLEFISEAIIHVLHSRHPGDFGADAQGAMNKALELFRKDIAAKY

hhhhh..
KELGYQG
```

In some way or another, this is similar to the structure of myoglobin (4mnb) in the Protein Data Bank [32] given below:

```
....hhhhhhhhhhhhhhh.hhhhhhhhhhhhhhhhhhhhhh........hhhhhhhhhhhhhhhhhhhh
..VLSEGEWQLVLHVWAKVEADVAGHGQDILIRLFKSHPETLEKFDRFKHLKTEAEMKASEDLKKHGVTVLTA
..1         11        21        31        41        51        61        71

hhhhhh........hhhhhhhhhh....hhhhhhhhhhhhhhhhhhh.....hhhhhhhhhhhhhhhhhhhh
LGAILKKKGHHEAELKPLAQSHATKHKIPIKYLEFISEAIIHVLHSRHPGDFGADAQGAMNKALELFRKDIAA
          81      91        101       111       121       131       141
hhhhh....
KYKELGYQG
     151
```

Where Blue-are hydrophilic and Violet-are hydrophobic amino acids.

Also for another comparison, we have run the sequence of myoglobin (4mbn) in the protein secondary structure prediction server APSSP2 of Raghava [32] and obtained the helix-turn-helix results in Figure 2 after we have considered the strand and coil states of Raghava's output as turns, that is, considering their helical probability equal to zero.

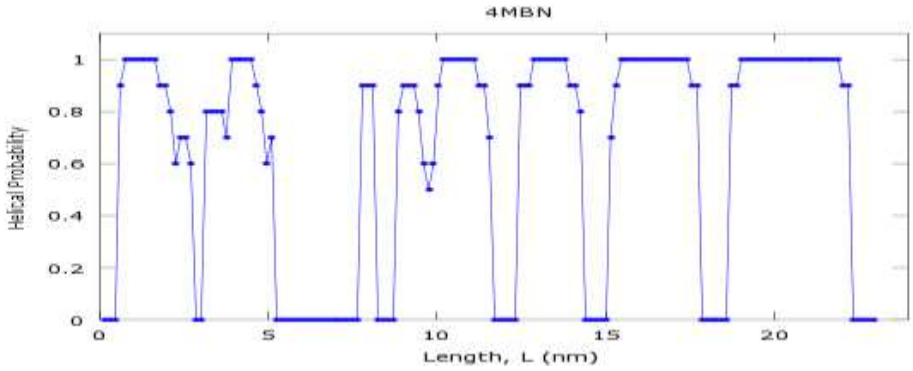

Figure 2: 4MBN: APSSP2 Results: Helical probability versus length where each dot represent an amino acid

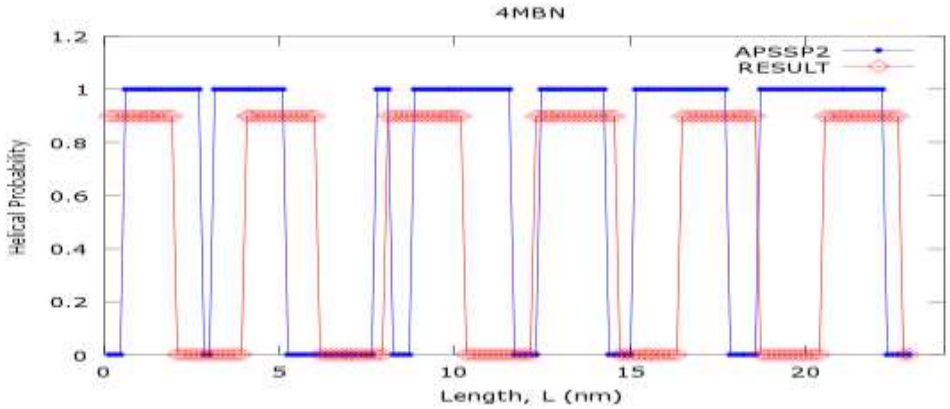

Figure 3: 4MBN: Helical probability versus length where each dot represents an amino acid

In order to give the reader a better idea of what we are trying to point out, we presented in Figure 3 a modified helix-turn-helix plot of our prediction (red curve) together with a modified helix-turn-helix prediction of APSSP2 (blue curve). In that figure, we replaced the non-zero values of helical probability with 0.9 for our prediction and replaced the non-zero values of helical probability with 1.0 for the APSSP2 prediction to show a rough comparison. As can be seen, APSSP2 predicted seven helical turns, which compared to literature APSSP2 has better and more realistic prediction because it employs a sophisticated Example Based Learning (EBL) approach together with a combination of neural network and nearest neighbour algorithm.

Our model, on the other hand predicted six equally spaced helical turns using Eq. (12) as the drift coefficient. Our present result does not quietly matched with the APSSP2 prediction but if we can correctly identify the right form of the drift coefficient for our model, we can have a faster and better prediction accuracy that is comparable to APSSP2 and other secondary structure prediction software or server. The main advantage of our model is that it can predict the structure of alpha helical protein in solvents very fast compared to other prediction methods. Especially we now have enormous amount of available data for proteins deposited in the Protein Data Bank. We can use the available data to constrain the form of the drift function. At the moment, with our chosen drift function (Eq. (12)), we closely predicted the structure of myoglobin (4mbn) and closely identified the amino acid sequence on the helical segments. To improve our prediction, we need to modify the form of Eq. (12), such as adding terms that account for the type of solvents where the protein is being immersed or another term that accounts for the properties of each amino acid (such as hydropathy index, charge, etc.) which are the focus of our future studies.

5 Conclusion

In conclusion, our results reveal the application of the winding probability function using the drift coefficient, $f(s) = k\sum_{q=1,3,5,\ldots}^{p}\cos(qvs)$. The helix-turn-helix structure of myoglobin (4mbn) and the amino acid sequence we predicted are comparable to the prediction of APSSP2 secondary structure prediction server and to PDB structure. The difference can be attributed to the drift coefficient used and can be improved with much less computing time compared to other computational methods. The results can be used to explore other α-helical proteins. The formation of helical and non-helical segments had been explored, and the question why this specific conformation is achieved for a protein to be biologically functional remains to be addressed however.

Acknowledgments. W. I. B. wishes to thank Dr. Christopher C. Bernido, Dr. Ma. Victoria Carpio-Bernido, and Dr. Jinky B. Bornales for helpful discussions and guidance on this research and acknowledges financial support from the Department of Science and Technology (DOST- ASTHRDP, Philippines).

References

[1] See, e.g., N. Y. Chen, Z. Y. Su and C. Y. Mou, Effective Potentials for Folding Proteins, *Phys. Rev. Lett.*, **96** (2006), 078103. http://dx.doi.org/10.1103/physrevlett.96.078103

[2] W. Yu, K. Chung, M. Cheon, M. Heo, K. H. Han, S. Ham and I. Chang, Cooperative folding kinetics of BBL protein and peripheral subunit-binding domain homologues, *Proc. Nat'l Acad. Sci. USA*, **105** (2008), 2397-2402. http://dx.doi.org/10.1073/pnas.0708480105

[3] See, e.g., J. S. Yang, S. Wallin and E. I. Shakhnovich, Universality and diversity of folding mechanics for three-helix bundle proteins, *Proc. Nat'l. Acad. Sci. USA*, **105** (2008), 895-900. http://dx.doi.org/10.1073/pnas.0707284105

[4] S. Wallin and E. I. Shakhnovich, Understanding ensemble protein folding at atomic detail, *J. Phys: Condens. Matter*, **20** (2008), 283101. http://dx.doi.org/10.1088/0953-8984/20/28/283101

[5] See, e.g., G. Chopra, C. M. Summa and M. Levitt, Solvent dramatically affects protein structure refinement, *Proc. Nat'l. Acad. Sci. USA*, **105** (2008), 20239-20244. http://dx.doi.org/10.1073/pnas.0810818105

[6] B. van den Berg, R. Wain, C. M. Dobson and R. J. Ellis, Macromolecular crowding perturbs protein refolding kinetics: implications for folding inside the cell, *The EMBO Journal*, **19** (2000), 3870-3875. http://dx.doi.org/10.1093/emboj/19.15.3870

[7] C. C. Bernido, M. V. Carpio-Bernido and M. G. O. Escobido, *Stochastic and Quantum Dynamics of Biomolecular Systems*, American Inst. of Physics, New York, 2008.

[8] H. Risken, *The Fokker-Planck Equation*, Springer-Verlag, Berlin, 1996. http://dx.doi.org/10.1007/978-3-642-61544-3

[9] C. Gardiner, *Handbook of Stochastic Methods*, 2nd ed., Springer-Verlag, Berlin, 1985.

[10] See, e.g., A. Inomata and V. A. Singh, Path integrals with a periodic constraint: Entangled strings, *J. Math. Phys.*, **19** (1978), 2318-2323. http://dx.doi.org/10.1063/1.523588

[11] See, e.g., S. F. Edwards, Statistical mechanics with topological constraints: I, *Proc. Phys. Soc. London*, **91** (1967), 513-519. http://dx.doi.org/10.1088/0370-1328/91/3/301

[12] S. Prager and H. L. Frisch, Statistical Mechanics of a Simple Entanglement, *J. Chem. Phys.*, **46** (1967), 1475. http://dx.doi.org/10.1063/1.1840877

[13] F. W. Wiegel, Entanglement probabilities for a harmonically bound macro-

molecule, *J. Chem. Phys.*, **67** (1977), 469-472.
http://dx.doi.org/10.1063/1.434891

[14] T. Hida, H. H. Kuo, J. Potthoff and L. Streit, *White Noise. An Infinite Dimensional Calculus*, Kluwer, Dordrecht, 1993.
http://dx.doi.org/10.1007/978-94-017-3680-0

[15] N. Obata, *White Noise Calculus and Fock Space*, Lecture Notes in Mathematics, Vol. 1577, Springer, Berlin, 1994.
http://dx.doi.org/10.1007/bfb0073952

[16] H. H. Kuo, *White Noise Distribution Theory*, CRC, Boca Raton, Florida, 1996.

[17] L. Streit and T. Hida, Generalized Brownian functionals and the Feynman integral, *Stoch. Proc. Appl.*, **16** (1983), 55-69.

[18] See, e.g., C. C. Bernido and M. V. Carpio-Bernido, Entanglement probabilities of polymers: a white noise functional approach, *J. Phys. A: Math. Gen.*, **36** (2003), 4247-4257.
http://dx.doi.org/10.1088/0305-4470/36/15/302

[19] L. S. Schulman, *Techniques and Applications of Path Integration*, Wiley, New York, 1981.

[20] M. G. Laidlaw and C. M. DeWitt, Feynman Functional Integrals for Systems of Indistinguishable Particles, *Phys. Rev*. D, **3** (1971), 1375-1378.
http://dx.doi.org/10.1103/physrevd.3.1375

[21] C. C. Bernido and M. V. Carpio-Bernido, Path integrals for boundaries and topological constraints: A white noise functional approach, *J. Math. Phys*., **43** (2002), 1728-1736. http://dx.doi.org/10.1063/1.1456254

[22] C. C. Bernido and A. Inomata, Path integrals with a periodic constraint: The Aharonov–Bohm effect, *J. Math. Phys*., **22** (1981), 715.
http://dx.doi.org/10.1063/1.524963

[23] A path moving clockwise, but no winding may be labeled by $n = 0^-$, and a path going counterclockwise with no winding by, $n = 0^+$.

[24] I. S. Gradshteyn and I. M. Ryzhik, *Table of Integrals, Series, and Products*, 5^{th} ed., Academic Press, San Diego, 1994.

[25] C. C. Bernido and M. V. Carpio-Bernido, Overwinding in a stochastic model of an extended polymer, *Phys. Lett. A*, **369** (2007), 1-4.

http://dx.doi.org/10.1016/j.physleta.2007.03.083

[26] C. C. Bernido, M. V. Carpio-Bernido and J. B. Bornales, On chirality and length-dependent potentials in polymer entanglements, *Phys. Lett. A*, **339** (2005), 232-236. http://dx.doi.org/10.1016/j.physleta.2005.03.037

[27] C. C. Bernido, M. V. C. Carpio-Bernido, White Noise Analysis: Some Applications in Complex Systems, Biophysics and Quantum Mechanics, *Int. J. Mod. Phys. B*, **26** (2012), 1230014. http://dx.doi.org/10.1142/s0217979212300149

[28] C. C. Bernido, M. V. Carpio-Bernido and H. P. Aringa, Topology-dependent Entropic Differences for Chiral Polypeptides in Solvents, *Phys. Lett. A*, **375** (2011), 1225-1228. http://dx.doi.org/10.1016/j.physleta.2011.01.030

[29] http://www.rcsb.org/pdb/explore/remediatedSequence.do?structureId=4MBN&bionumber=1 Retrieved October 10, 2014.

[30] W. I. Barredo, C. C. Bernido, J. B. Bornales and H. P. Aringa, On the Diffusion of Alpha-Helical Proteins in Solvents, *Int. J. Mod. Phys. Conf. Ser.*, **36** (2015), 1560018. http://dx.doi.org/10.1142/s2010194515600186

[31] http://www.ebi.ac.uk/pdbe-site/pdbemotif/sequence?accessionCode=4mbn Retrieved April 2, 2014.

[32] G. P. S. Raghava, APSSP2: A combination method for protein secondary structure prediction based on neural network and example based learning, CASP5. A-132, 2002.

Received: February 15, 2016; Published: March 25, 2016